

# Implementation and Evaluation of an IPT battery charging system in assisting Grid Frequency Stabilisation through Dynamic Demand Control

Chang-Yu Huang, *Student Member IEEE*, John T. Boys, Grant A. Covic, *Senior Member IEEE*, Josh R. Lee, *Student Member IEEE*, Richard V. Stebbing, *Student Member IEEE*  
The University of Auckland  
Department of Electrical and Computer Engineering  
Private Bag 92019, Auckland 1142, New Zealand  
Tel: +64 (9) 373-7599, Ext: 88159, Fax: +64 (9) 373-7461  
[changyu.huang@gmail.com](mailto:changyu.huang@gmail.com)

**Abstract**—The paper presents a hands free Inductive Power Transfer (IPT) system for charging Electric Vehicle (EV) batteries using a technique called dynamic demand control (DDC). A typical IPT system comprises a power supply, a pair of magnetic pads for wireless power coupling and a power regulator to drive the load as required. DDC enables suitable domestic appliances to assist grid stabilisation by adjusting their power demand according to the utility frequency variation. This paper explains the conceptual design of a wireless power charging system that includes DDC and details the experimental set up for an emulated erratic isolated power network which combines a variable speed drive, an induction motor and an AC generator. The measured performance of the emulated power network generator frequency without DDC varies between 47 Hz to 53Hz, but this same network frequency is maintained within a preset window of 49.5 Hz to 50.5 Hz when DDC is activated in the IPT battery charging system. Consequently EV charging systems employing DDC control could potentially act as a grid stabilising load, enabling increased penetration of fluctuating sources of energy (such as wind) in the generation mix.

**Key words:** Inductive Power Transfer, Electric Vehicle battery charging, Dynamic Demand Control

## I. INTRODUCTION

Since the latter half of the 20th century, there have been increasing demands on developing vehicles utilizing an environmentally friendly power source to replace the conventional internal combustion engine (ICE). Battery electric vehicles (BEVs), as one of the candidates to replace the ICE, have been under continuous research and development cycles for decades. This increase in popularity of BEVs is likely to generate a new type of energy storage load on the power system grid. In New Zealand previous research indicates that with large scale deployment of BEVs, the electricity requires to charge BEVs could be between 10-20% of current NZ electricity generation [1]. As EV battery charging is flexible and does not need to operate at constant power levels, it could be used (with suitable charging infrastructure) as a means to assist grid stabilization.

Dynamic Demand Control (DDC), as proposed in [2], is a method of adjusting the power demand of suitable domestic appliances based on the state of the utility power network. The rationale behind DDC is that domestic appliances can use the utility frequency as a measure of the power system stability and adjust their demand accordingly. In essence, when the demand for power exceeds supply, the supply frequency decreases and as a means of compensation each domestic appliance should decrease its power consumption. In this way, home appliances can work towards stabilizing the power network, reducing the required governor activity of spinning reserve generator and increasing the penetration of time variable renewable energy sources [3]. A hands free inductive power transfer (IPT) system transfers power efficiently across an air gap. It is regarded as one of the most promising means for delivering power to an EV for both stationary and high way charging due to its robustness and safety [4].

The focus of this work is to implement and evaluate the performance of a 1.5 kW IPT battery charging system with dynamic demand control in an emulated isolated power network with erratic behavior similar to a time-variable renewable energy source like a wind turbine. In this system, a single phase IPT power supply with minimal DC energy storage presented in [5] is used because it has good input mains power factor ( $\text{pf} = 0.94$ ) and efficiency. The IPT pick-up controller used in this system is an LC parallel tuned AC-AC controller as presented in [6]. The advantage of this topology is fast response, good efficiency and the ability to regulate its output power on a continuous basis. With the implementation of DDC, the pick-up output power should vary according to the grid frequency within a preset window. The set up for evaluating DDC is using a variable speed drive (VSD), a 3 phase induction machine and a 3 phase AC generator to emulate a standalone power system network with a maximum power of 7 kW. The overall system set-up is discussed in detail and the overall battery charging system

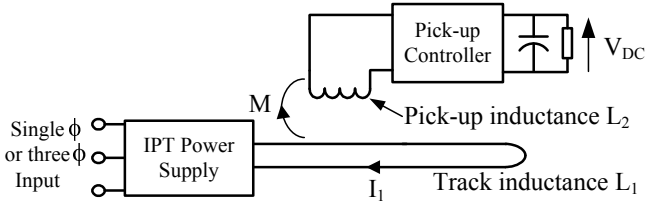


Fig. 1. Conceptual Diagram of IPT system

performance with DDC is presented along with measured results.

## II. SYSTEM OVERVIEW

### A. IPT Fundamental

A typical IPT system is shown schematically in Fig. 1. Notably there are two conceptually different parts to the system with galvanic isolation between them: a power supply takes power from a utility and converts it to a current at VLF frequency (in the range 5-50 kHz) which is used to energize an elongated loop or a lumped coil called a track, and one or more pick-ups couple power inductively from the track. These pick-ups are tuned or compensated with capacitors and power from them is then regulated and available to drive loads as required. As there is no physical contact between the primary and secondary coils, an IPT system is very resilient to chemical, water and dirt, and the secondary pick-up has good lateral movement tolerance relative to the primary track [7]. For these features, IPT systems are now widely used in a variety of industrial applications. Examples include, material handling systems, clean room applications and battery charging for people movers and electric buses [8-11].

### B. System Overview

The proposed IPT battery charging system with dynamic demand control is shown conceptually in Fig. 2. The IPT power supply, presented in [5], is used in this system because it has good efficiency and good input mains power factor. In order to perform DDC the pick-up controller topology needs to be able to regulate its output power on a continuous basis or in multiple small steps like those discussed in [6, 12, 13]. An LC parallel tuned AC-AC pick-up controller presented in [6] is used simply because it has high efficiency and fast

response, and the capability to vary the output power continuously from no load to full load. The primary and secondary coils used in this system (referred herein as charger pads) are circular lumped coil types as presented in [10, 14]. This pad configuration is one of the most practical for vehicle battery charging applications due to their efficiency and ability to constrain leakage flux [12].

The role of the dynamic demand controller is to send the desired output power level to the pick-up controller based on the measured grid frequency. The frequency window used in this system is set but not limited to 49.5 – 50.5 Hz. In this range, the battery charging system should operate linearly from no load to full power of 1.5 kW as demonstrated in Fig. 3. As the primary track current envelope is amplitude modulated at a multiple of the utility frequency, the induced voltage in the secondary is also modulated enabling the grid frequency to easily be measured at the secondary side without complicated circuitry. For systems with constant track current envelopes, an IPT communication technique as discussed in [15] could be used to transmit the grid frequency information to the dynamic demand controller from the power supply without adding additional dedicated wireless communication devices.

### C. Theoretical Aspects

A simple block diagram of the global system is shown in Fig. 4. It comprises the power network/generator (without any governor action) and the battery charging system. In the block diagram, the power network is simply modeled as a rotational body with inertia  $J$  ( $\text{Nm}^2$ ), and “ $k$ ” is the droop factor ( $\text{Nm}/(\text{rad}/\text{sec})$ ), which is essentially the slope of the line in Fig. 3. For the example shown, the line rises from zero to rated torque in 1Hz or 2% of rated speed. For a 2-pole generator rated at 7.5 kW, “ $k$ ” would be 25  $\text{Nm}/3.14$  radians/sec or approximately 8  $\text{Nm}/(\text{rad}/\text{sec})$ .  $T$  is the frequency measurement time constant and as shown is assumed to be that of a first order system. These figures are for the 2-pole equivalent of the machine and generator used for the laboratory measurements described in Section IV. Without the battery charging system, any torque variation ( $\Delta\tau$ ) applied to the generator results in a system frequency

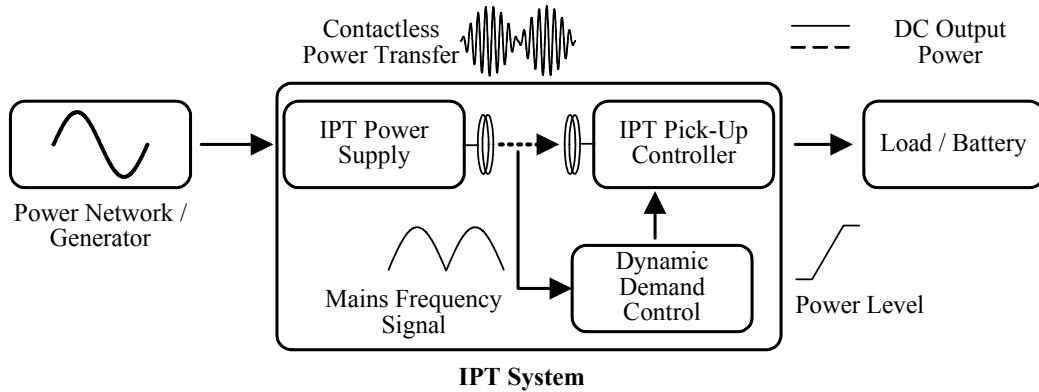


Fig. 2. Overview block diagram of the IPT charging system

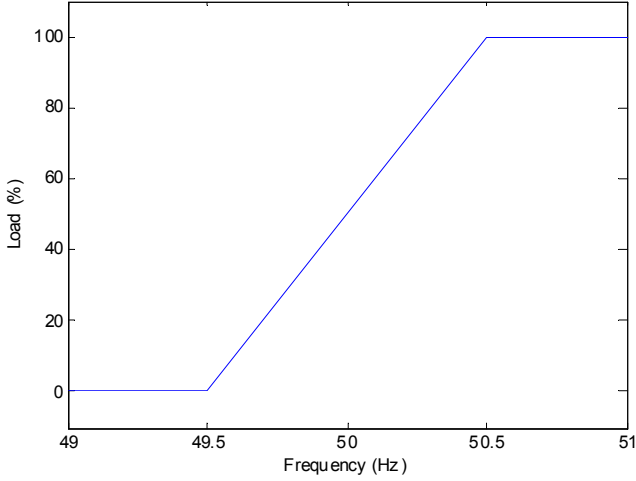


Fig. 3. Output power and frequency characteristic of DDC

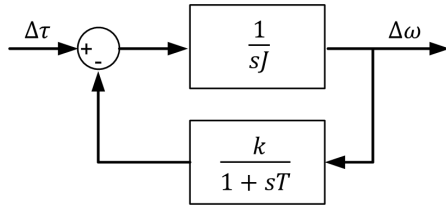


Fig. 4. Block diagram of the global system with the generator (top) and the charging system (bottom)

deviation ( $\Delta\omega$ ) (assuming constant consumer loading condition). Using the dynamic demand control IPT system,  $\Delta\tau$  is then reduced from the power network/generator by varying the power delivered to the load/battery according to  $\Delta\omega$ . This results in an appropriate change to the grid frequency that maintains the frequency within the preset window.

In a practical application (Fig. 4) a change in torque  $\Delta\tau$  causes a change in the speed  $\Delta\omega$  of the wind turbine giving a change in the frequency of the generated voltage. The turbine is assumed to have no other governing device so the change in torque causes the speed to continue to increase. The frequency of the generated voltage is measured, and filtered by a simple first order filter, and used to switch on an increased electrical load that reduces the net change in torque applied to the wind turbine.

Using the usual symbols for torque speed etc. the transfer function for the change in speed to a change in torque is given by:

$$\frac{\Delta\omega}{\Delta\tau} = \frac{1+sT}{s^2JT+sJ+k} \quad (1)$$

For this system the damping factor, settling time, and steady state error are given by

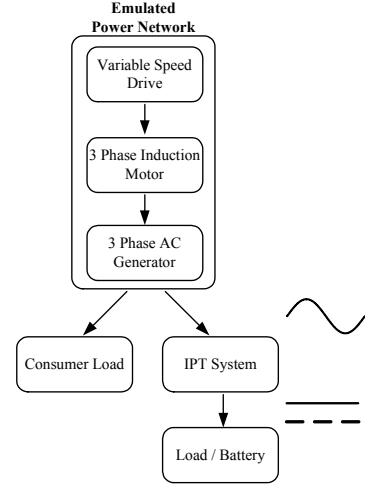


Fig. 5. Overview block diagram of the IPT charging system

$$\zeta = \frac{1}{2} \sqrt{\frac{J}{Tk}} \quad (2)$$

$$t_s \approx \pi \sqrt{\frac{JT}{k}} \quad (3)$$

$$\Delta\omega = \frac{\Delta\tau}{k} \quad (4)$$

Thus for the 2-pole generator as above, assuming a small system inertia of  $0.7\text{kgm}^2$  and a 100 ms filter time constant, the damping factor is 0.47, the settling time is approximately 0.3 s and the speed offset is 0.125 radian/sec per Nm.

This example has highlighted a tiny system – corresponding to the experimental example given below. Larger systems would have much higher inertias giving better damping factors but the same offset dependent on the slope of the line in Fig. 3. To get faster response the measurement time constant may be reduced but this leads to a significantly worse damping factor.

### III. IMPLEMENTATION OF THE IPT SYSTEM AND DYNAMIC DEMAND CONTROLLER

#### A. IPT Power Supply

The power supply, presented in [5], is used in the proposed dynamic demand control IPT battery charging system, and outputs a controlled voltage (and a regulated current) at a fixed frequency of 20 kHz into a series-parallel LCL resonant network topology. This power supply has minimal DC energy storage, good input mains power factor and efficiency. It is mainly designed for single phase mains application. The

feature of this power supply is that the DC link in the power supply and hence the track current  $I_1$  amplitude modulates at twice the mains frequency due to the lack of minimal DC energy storage.

### B. IPT Pick-up Controller

The pick-up topology, shown in Fig. 6, is called an LC parallel tuned AC processing pick-up controller [6]. The switching controller, comprises two back to back MOSFETs to form an AC switch that operates synchronously at the IPT frequency. The AC switch together with two diodes perform rectification to produce a regulated dc output to the load through the dc inductor  $L_{dc}$ . The output power from the LC resonant tank is regulated by the resonant tank voltage clamp time, shown in Fig. 7, generated by the AC switching of  $S_1$  and  $S_2$ . Because the AC switches operate at ZVS, it makes the AC processing pick-up very efficient [6].

### C. Dynamic Demand Controller

As discussed in the previous section, the role of the DDC controller is to measure the utility frequency and instruct the AC processing controller to control the output power level at a value suitable for stabilising the generator and maintaining its frequency to be within a preset range. (in this case 49.5 Hz to 50.5 Hz.)

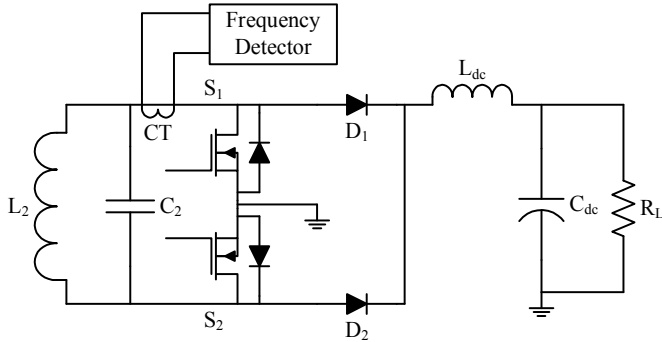


Fig. 6. Circuit diagram of an IPT AC processing pick-up controller with frequency detector.

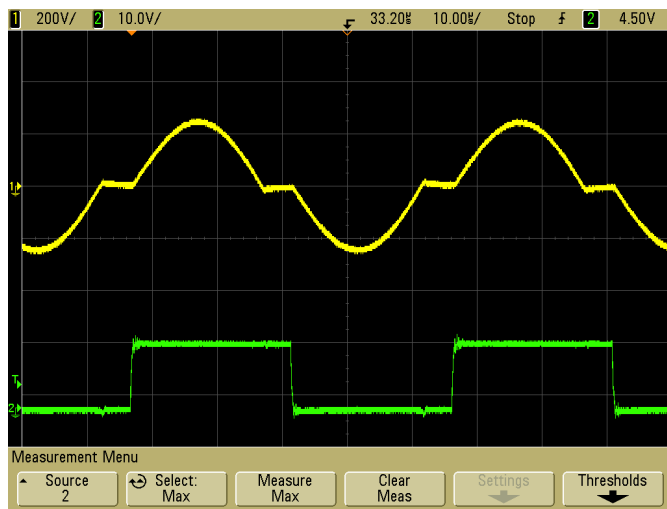


Fig. 7. Top trace: LC resonant tank voltage across  $L_2$  and  $C_2$ . Bottom trace: gate drive waveform for  $S_2$ .

In an IPT system, due to the physical isolation between the primary and secondary controller the utility frequency is not directly accessible by the DDC controller. Traditionally it would require the primary power supply to perform the frequency measurement and to transmit the information to the pick-up controller by means of wireless communication. However, a convenient feature of the power supply used in the proposed system is that its track current ( $I_1$ ) amplitude modulates at twice of the utility frequency as described previously. This provides an easy means of measuring the utility frequency within the DDC controller. The output current of the LC resonant tank on the pick-up stays relatively constant irrespective of the load. Hence the utility frequency deviation can be monitored by the DDC using a current transformer, shown in Fig. 6, together with peak detector and filter (Fig. 8) to detect the pick-up resonant tank envelope frequency, which is then synchronised to the utility frequency.

To measure the performance of the frequency measurement technique, the proposed battery charging system is driven from a single phase variable frequency AC supply (Agilent AC power source 6813B) with the system operating under full power condition. The frequency was varied slowly from 49.5 Hz to 50.5 Hz. Partial measured results are presented in Fig. 9. It can be seen that individual measurements are affected by noise. To improve this, the measured results are filtered using a rolling average of eight measurements. The result (in the bottom trace of Fig. 9) shows that a frequency variation of 0.01 Hz is now discernible.

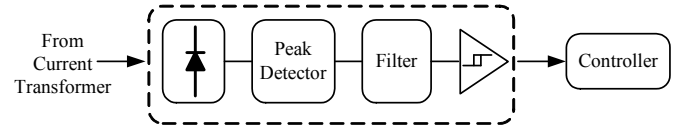


Fig. 8. Block diagram of frequency measurement process

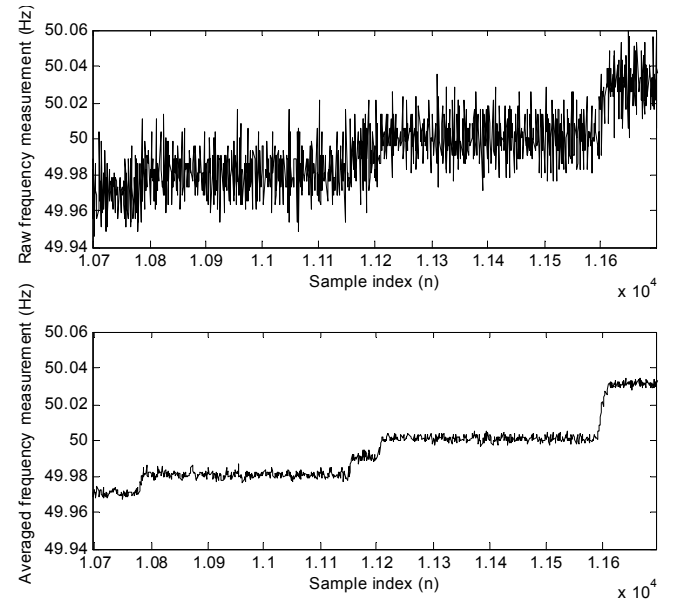


Fig. 9: Raw frequency measurements (top) and averaged frequency measurements (bottom)

#### IV. PERFORMANCE OF DDC IPT CHARGING SYSTEM AND DISCUSSION

##### A. Experimental Set-up

For evaluating the performance of the dynamic demand control IPT system, a programmable standalone power generation system was constructed comprising a variable speed drive (VSD), a 3 phase induction motor and a 3 phase AC generator as shown in Fig. 5. This system was set up to generate 230 V 50 Hz (per phase) and is capable of delivering up to 7 kW total. The IPT system was connected to one phase, while constant resistive loads were connected to the remaining two phases to emulate a constant consumer load demand.

To emulate a power network with high penetration of time-variable renewable energy sources like wind energy, the VSD was configured to operate the induction motor in a torque-limited state. In this state the desired speed is set to the maximum value but the actual speed is limited by the torque limit. Changes to the torque-limit cause the generator to accelerate or decelerate. A random but repeatable pattern of torque commands with a distribution close to a Weibull pdf was used as the torque input to the VSD as shown in the top trace of Fig. 10. In this way a highly variable isolated power system was created with the ideal feature that the numerical sequence could be repeated to make different measurements on the same data.

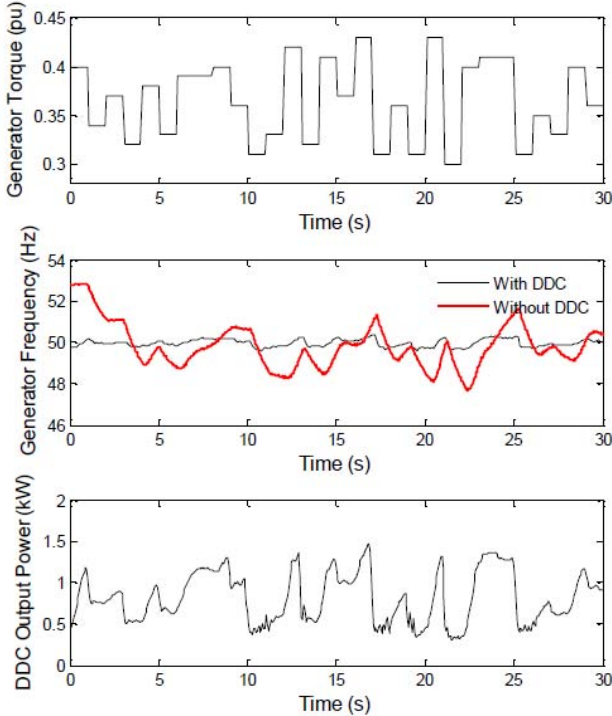


Fig. 10: Measured generator frequency and charging system output power (middle and bottom) when the motor-generator set is driven with a random torque pattern (top)

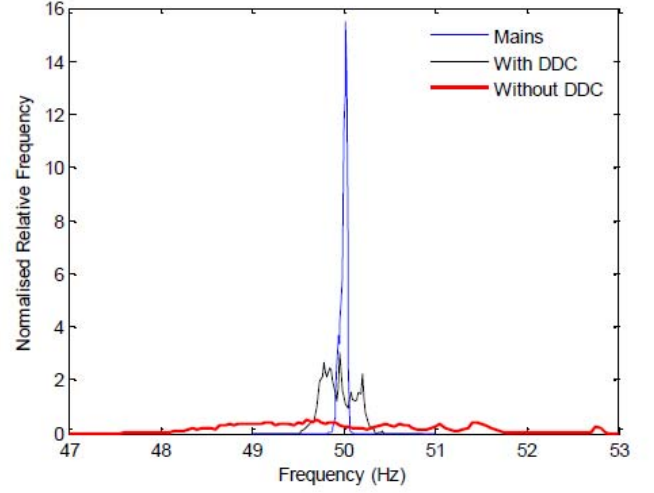


Fig. 11: Distribution of the generator frequency with and without dynamic demand controller

##### B. Practical Results

The system was operated in a steady-state mode and a sequence of 50 random torque patterns was input to the VSD at one second intervals to emulate wind power network. With the dynamic demand IPT battery charging system connected to the generator, the system frequency of the generator and the output power of the charging system were then measured under battery charging conditions. Using identical torque patterns, the system frequency was also measured with the battery charger behaving like a static load (without DDC). The measured results from the 30 second samples for both experiments are shown in Fig. 10, while the measured frequency distributions are presented in Fig. 11.

Without DDC in place, the measured generator frequency is unstable and varies from 47 Hz to 53 Hz. By any measure this is a power supply of very low quality and has limited usefulness. By comparison, with DDC employed (as shown on the same traces of Fig. 10 and 11 for comparison), the frequency of the generator is successfully maintained within the preset window of 49.5 to 50.5 Hz. A comparison of the torque pattern input to the generator and the output power profile of the charging system clearly shows how closely the output power profile follows the input torque pattern. As the torque limit of the induction motor is increased, the frequency speeds up but the charging system absorbs this excess power and removes the excess torque from the generator to roughly maintain the system frequency. Conversely, as the torque limit is decreased, the generator slows down forcing the charging system to reduce its power consumption, thereby reducing the total frequency change.

##### C. Discussion

The measured results of the dynamic demand control experiment with an emulated fluctuating power network clearly demonstrate how a 1.5 kW DDC controlled IPT battery charger connected to a 7 kW standalone generator can

offer considerable frequency smoothing by adjusting its output power according to deviations in the supply frequency. Although the frequency window is set here from 49.5 Hz to 50.5 Hz for ease of implementation, this could easily be adjusted as required to suit any network. In consequence a large scale deployment of BEVs having chargers that operate under DDC could act as a controlled distributed load that automatically improves the stability of any supply network, without the need for complicated high bandwidth centralised communication infrastructures, reducing the required governor activity of spinning reserve and increasing the wind power penetration without significant increase of grid demand-supply balancing cost. However, care needs to be taken to consider the regional supply-and-demand balance to prevent unwanted increase of Tie-line flow as discussed in [16].

## V. CONCLUSION

The idea of using an IPT EV battery charging system to perform dynamic demand control to assist in grid stabilisation is explained from both a system overview and a theoretical perspective in this paper. A 1.5 kW IPT battery charging system prototype cooperating with dynamic demand controller is presented. This system was tested with an emulated power network which comprises a variable speed drive, a three phase induction motor and a three AC generator. The emulated power network was set up to emulate a wind turbine which outputs irregular power with time. The system performance measurements showed that the frequency of this power network varied from 47 Hz to 53 Hz with no DDC action in the pick-up controller while the frequency of the generator was maintained within 49.5 Hz to 50.5 Hz with the DDC action applied. This indicates that having EV chargers that operate under DDC will behave as a controlled distributed load that could assist in grid stabilisation.

## ACKNOWLEDGMENT

The authors would like The University of Auckland Doctoral Scholarship and the UniServices Ltd for sponsoring the research.

## REFERENCES

- [1] M. Duke and T. Anderson, "The potential for Battery Electric Vehicles in New Zealand," in *Energy, Transport and Sustainability Symposium, Wellington, New Zealand, 2008*.
- [2] F. C. Schweppe, "A Frequency Adaptive, Power-Energy Re-scheduler," U.S. patent 4317049.
- [3] J. A. Short, D. G. Infield and L. L. Freris, "Stabilization of Grid Frequency Through Dynamic Demand Control," *Power Systems, IEEE Transactions on*, vol. 22, no. 3, pp. 1284-1293, 2007.
- [4] A. Brooker, M. Thornton and J. Rugh, "Technology Improvement Pathways to Cost-Effective Vehicle Electrification", in *SAE 2010 World Congress, Detroit, Michigan April 13-15 2010*.
- [5] J. T. Boys, C. Y. Huang and G. A. Covic, "Single-phase unity power-factor inductive power transfer system," in *Power Electronics Specialists Conference, Rhodes, 2008*, pp. 3701-3706.

- [6] H. H. Wu, J. T. Boys and G. A. Covic, "An AC Processing Pickup for IPT Systems," *Power Electronics, IEEE Transactions on*, vol. PP, no. 99, pp. 1-1, 2009.
- [7] G. A. Covic, J. T. Boys, M. L. G. Kissin and H. G. Lu, "A Three Phase Inductive Power Transfer System for Roadway Powered Vehicles," *IEEE Trans. Ind. Electron.*, vol. 54, no. 6, pp. 3370-3378, 2007.
- [8] J. L. Villa, J. Sallán, A. Llombart and J. F. Sanz, "Design of a high frequency Inductively Coupled Power Transfer system for electric vehicle battery charge," *Applied Energy*, vol. 86, no. 3, pp. 355-363, 2009.
- [9] G. A. Covic, G. Elliott, O. H. Stielau, R. M. Green and J. T. Boys, "The design of a contact-less energy transfer system for a people mover system," in *Proceedings International Conference on Power System Technology, Perth, Australia, 2000*, pp. 79-84.
- [10] Y. Kamiya, M. Nakaoka, T. Sato, J. Kusaka, Y. Daisho, S. Takahashi and K. Narusawa, "Development and performance evaluation of advanced electric micro bus equipped with non-contact inductive rapid-charging system," in *23rd International Electric Vehicle Symposium, Anaheim, USA, 2007*, pp. 1-14.
- [11] J. L. Villa, J. A. Sallan, A. Llombart and J. F. Sanz, "Practical Development of a 5 kW ICPT System SS Compensated with a Large Air gap," in *IEEE International Symposium on Industrial Electronics, 2007*, pp. 1219-1223.
- [12] C.-Y. Huang, J. T. Boys, G. A. Covic and M. Budhia, "Practical considerations for designing IPT system for EV battery charging," in *Vehicle Power and Propulsion Conference, 2009. VPPC '09. IEEE, 2009*, pp. 402-407.
- [13] J. T. Boys, C. I. Chen and G. A. Covic, "Controlling Inrush Currents in Inductively Coupled Power Systems," in *7th International Power Engineering Conference, Singapore, 2005*, pp. 1-6.
- [14] M. Budhia, G. A. Covic and J. T. Boys, "Design and optimisation of magnetic structures for Lumped Inductive Power Transfer System," *IEEE Energy Conversion Congress and Exposition accepted for publication*.
- [15] E. L. v. Boheemen, J. T. Boys and G. Covic, "Dual-tuning IPT systems for low bandwidth communications," in *IEEE Conference on Industrial Electronics and Applications, Harbin, China, 2007*, pp. 586-591.
- [16] M. Takagi, K. Yakaji, H. Yamamoto, "Power System Stabilization by charging power management of Plug-in Hybrid Electric Vehicles with LFC signal", in *Vehicle Power and Propulsion Conference, 2009, VPPC '09. IEEE, 2009*, pp. 822-826